



CHORUS

This is the accepted manuscript made available via CHORUS. The article has been published as:

## Ultrabroadband Microresonators with Geometrically Nonlinear Stiffness and Dissipation

Randi Potekin, Keivan Asadi, Seok Kim, Lawrence A. Bergman, Alexander F. Vakakis, and  
Hanna Cho

Phys. Rev. Applied **13**, 014011 — Published 8 January 2020

DOI: [10.1103/PhysRevApplied.13.014011](https://doi.org/10.1103/PhysRevApplied.13.014011)

## **Ultra-broadband Microresonators with Geometrically Nonlinear Stiffness and Dissipation**

Randi Potekin<sup>1</sup>, Keivan Asadi<sup>2</sup>, Seok Kim<sup>1</sup>, Lawrence A. Bergman<sup>3</sup>, Alexander F.  
Vakakis<sup>1</sup>, Hanna Cho<sup>2</sup>

<sup>1</sup> Department of Mechanical Science and Engineering,  
University of Illinois, Urbana-Champaign, IL 61820, USA

<sup>2</sup> Department of Mechanical and Aerospace Engineering,  
The Ohio State University, Columbus, OH 43210, USA

<sup>3</sup> Department of Aerospace Engineering,  
University of Illinois, Urbana-Champaign, IL 61820, USA

In the area of micro/nanoresonant sensing, energy harvesting, and signal processing, the ability to provide resonance over a broad frequency bandwidth has been a persistent goal. One strategy for a broadband resonator that researchers focus on is to exploit the relatively large-amplitude response of micro/nanoresonators operating in the geometrically nonlinear dynamic regime. Geometric nonlinearity is well-known to have a hardening effect on the resonance curve thereby generating a broadband resonance, the bandwidth of which is limited by the linearized resonant frequency (lower bound) and the drop-down bifurcation frequency (upper bound). All else held constant, increasing the drop-down bifurcation frequency in the frequency response of a nonlinear resonator enhances the broadband resonance. In this work, ultra-broadband resonance of microresonators having geometrically nonlinear stiffness is investigated and validated experimentally. Specifically, a microresonator having cubic stiffness nonlinearity is excited at its base and as the excitation amplitude approaches a critical level, a sudden and significant increase in the resonant bandwidth of the fundamental bending mode is observed. The significant implications of this nonlinear phenomenon in sensing, signal processing and other applications in the microscale are discussed.

## I. INTRODUCTION

Many micro-electro-mechanical systems (MEMS) utilize a micromechanical resonator under harmonic excitation, undergoing either torsional or flexural vibrations [1]. Typically, one or more vibrational modes are driven and transduced into an electrical signal, which serves to provide the essential functionality of resonator-based MEMS. The harmonic excitation may be applied at the base or directly to the structure from a variety of different actuation forces including piezoelectric, electrostatic and magnetic. Traditionally, these resonators were designed and studied within the framework of linear dynamics, and researchers focused on mitigating sources of incidental nonlinearity [2-4]. Over the past couple of decades, a new approach to nonlinearity in micro/nanoresonators has emerged and is now an expanding, active research area. In this approach, *nonlinearity is intentionally incorporated* into the device design in order to leverage the rich nonlinear behavior for practical purposes [5-8].

Considering the design of microresonators, in the ongoing thrust for enhanced functionality, the size of state-of-the-art resonant MEMS is becoming increasingly small. When the relative response amplitude compared to the characteristic size of the device becomes large, axial strain along the beam induces a nonlinear restoring force in the resonator [9]. Specifically, geometric nonlinearity associated with mid-plane stretching in the beam generates a cubic stiffness term in the equation governing the response of the fundamental bending vibration mode (i.e., the motion is characterized by the Duffing equation). In this sense, all beam structures have a threshold amplitude above which they behave nonlinearly. As the characteristic size of the resonator decreases, this threshold amplitude decreases as well, and in extreme cases the linear dynamic regime may occur entirely below the noise floor. Accordingly, by operating at larger amplitudes that are well within the nonlinear regime, the signal-to-noise-ratio (SNR) may be enhanced, which is one source of motivation for investigating and implementing intentional nonlinearity in microelectromechanical (MEM) sensors and time-keeping devices [10-16]. The broadband resonance associated with geometric hardening can also be utilized in MEMS energy harvesting and bandpass filtering applications. A common issue in MEM energy

harvesting is frequency mismatch between the vibration source and the MEM harvester and, hence, resonant bandwidth expansion of the harvester can amplify the resulting output power [17-20]. It has also been shown that, through strategic design and/or coupling of Duffing oscillators, the nonlinear frequency response can be exploited to generate a nearly ideal bandpass MEM filter [21-23]. Furthermore, in certain applications, intentional nonlinear phenomena may result in paradigm-shifting improvements in the area of micro/nanoresonant sensing [24-39]. This new approach based on intentional utilization of nonlinearity, however, dictates predictive design and careful study of the dynamics in order to determine accurately the ranges of desirable and robust operation, thus avoiding unwanted effects (e.g., chaotic motions or dynamic instabilities) which can occur in nonlinear systems under external or parametric excitation [9, 40, 41].

It is a well-known result that cubic nonlinearity in a hardening Duffing oscillator causes forward bending of the resonance curve resulting in a broadband resonance. This contrasts to the classical narrowband Lorentzian resonance of a linear oscillator. For a fixed forcing level, the range of frequencies that constitutes the broadband resonance of a Duffing oscillator is determined by the linearized frequency (lower bound) and the drop-down bifurcation frequency (upper bound). In a recent study [16], it was shown that, for a clamped-clamped microcantilever subject to harmonic base excitation, there exists a critical excitation amplitude above which there is no theoretically predicted drop-down bifurcation frequency, yielding *ultra-broadband nonlinear resonance*. Physically, of course, it is not feasible to truly have no drop-down bifurcation in the frequency response curve. In practice, the inevitable drop-down bifurcation may occur due to various effects or unmodeled dynamics, e.g., the excitation of internal resonances yielding nonlinear energy transfers through modal interactions [10], shrinking of the domain of attraction of the upper (stable) resonance branch, perturbations of initial conditions due to noise, and/or nonlinear dissipative effects [42].

In this letter we present experimental evidence of ultra-broadband resonances in a flexible microresonator with cubic stiffness nonlinearity under harmonic base excitation. Specifically, we find that as the excitation amplitude approaches a critical level, the

resonant bandwidth of the fundamental bending mode suddenly increases substantially. This behavior is observed experimentally for two different microresonator systems. Further, we theoretically reconstruct the experimental resonance curves using a model having cubic stiffness nonlinearity and a two-phase damping model: linear damping is assumed for relatively low amplitudes whereas nonlinear damping proportional to the product of the displacement and the square of the velocity is assumed for large amplitudes. Good quantitative agreement between the experimental and theoretically reconstructed resonance curves is observed. Ultimately the ultra-wide broadband resonance could be exploited in MEM sensing, energy harvesting and filtering applications.

## II. THEORETICAL PREDICTION OF ULTRA-BROADBAND RESONANCES

We consider a single-degree-of-freedom (SDOF) Duffing oscillator with hardening cubic nonlinearity under harmonic base excitation. In previous works, e.g., [45], [47], it has been shown that such physics-based stiffness nonlinearity arises from geometric effects (nonlinear stretching) of a linear spring-damper element undergoing transverse oscillations (cf. also the following experimental section). The corresponding governing equation of motion, in non-dimensional form, is given by,

$$\hat{y}'' + 2\zeta_1\hat{y}' + \hat{y} + \alpha\hat{y}^3 = \hat{a}\Omega^2 \cos\Omega\tau \quad (1)$$

where  $\hat{y}$  is the displacement,  $\hat{a}$  the base excitation amplitude,  $\Omega$  the drive frequency,  $\zeta_1$  the linear damping coefficient, and  $\alpha$  the cubic stiffness coefficient, with all coefficients and variables being nondimensionalized.

In an effort to recover the drop-down frequency as a function of excitation amplitude for this system, we employ harmonic balance analysis [9]. Specifically, we assume an approximate one-term harmonic expansion of the displacement,  $\hat{y} = \hat{A}\cos(\Omega\tau - \varphi)$ , and balance the first (leading) harmonic in (1) to obtain the following approximate frequency-

amplitude relationship, omitting the higher harmonics in the response which are assumed to be negligible in the frequency range of interest:

$$\frac{3}{4}\alpha\hat{A}^3 = (\Omega^2 - 1)\hat{A} + \sqrt{\hat{a}^2\Omega^4 - (2\zeta_1\Omega\hat{A})^2} \quad (2)$$

The drop-down bifurcation point, i.e., the frequency where a “jump” from the upper stable resonance branch to the lower (linearized) branch occurs, can be estimated as the intersection of the frequency-amplitude curve defined by (2) and the so-called *backbone curve* [9, 37]. By definition, the backbone curve is the frequency-amplitude relationship corresponding to the system without damping ( $\zeta_1 = \zeta_2 = 0$ ) and external excitation ( $\hat{a} = 0$ ), and hence, from (2) is given by:

$$\frac{3}{4}\alpha\hat{A}^3 = (\Omega^2 - 1)\hat{A} \quad (3)$$

By combining (2) and (3), an equation defining the drop-down bifurcation frequency,  $\Omega_d$ , is recovered as follows:

$$\Omega_d = 1 / \sqrt{1 - \frac{3\alpha\hat{a}^2}{16\zeta_1^2}} \quad (4)$$

From (4), we see that for fixed system parameters, the drop-down frequency is real-valued only for excitation amplitudes below the critical level of  $\hat{a}_{\text{critical}} = \sqrt{16\zeta_1^2 / (3\alpha)}$ . For excitation levels above this critical level, there is no theoretically predicted drop-down bifurcation in the resonance curve. Physically, there must be drop-down bifurcations for excitation levels above the critical level but they are not captured by equation (1). In other words, the inevitable drop may be caused by unmolded dynamics such as the excitation of internal resonances [10], shrinking of the domain of attraction of the upper (stable)

resonance branch, perturbations of initial conditions due to noise, and/or nonlinear dissipative effects [42].

The drop-down frequency as a function of excitation amplitude is plotted in Fig. 1 for a Duffing oscillator with a linear resonant frequency of  $f_0 = 51\text{kHz}$ , a  $Q$ -factor of  $Q = 1/(2\zeta_1) = 1,515$  and a nondimensional cubic stiffness of  $\alpha = 9,173$ . For these parameters the critical excitation amplitude is  $\hat{a}_{\text{critical}} = 8.1 \times 10^{-6}$ . Here we see that the drop frequency increases at an increasing rate as the excitation amplitude increases and as the excitation amplitude approaches the critical level, the drop frequency increases without bound. In a physical system, it is not reasonable to expect the drop frequency to increase up to several orders of magnitude as shown in Fig. 1b, but we should expect to see that drop frequency increase suddenly and substantially as the excitation amplitude approaches the critical level.

To better understand this nonlinear dynamical phenomenon from a physical perspective, it is constructive to consider the case where harmonic excitation applied directly to the oscillator rather than to the base. The equation of motion in this case is,

$$\hat{y}'' + 2\zeta_1 \hat{y}' + \hat{y} + \alpha \hat{y}^3 = q \cos \Omega \tau \quad (5)$$

where  $q$  is the fixed forcing level. The drop-down frequency is then given by:

$$\Omega_d = \sqrt{\frac{1}{2} \left( 1 + \sqrt{1 + \frac{3\alpha q^2}{4\zeta_1^2}} \right)} \quad (6)$$

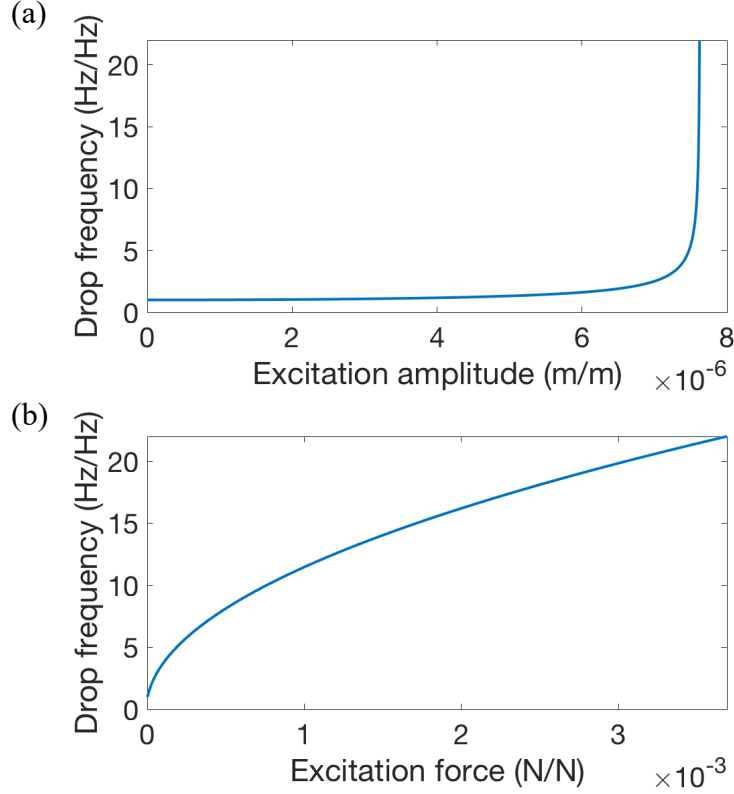


Figure 1. Computational curve of the drop-down frequency as a function of the excitation (a) amplitude and (b) force for a Duffing oscillator under harmonic (a) base excitation and (b) direct excitation. These results correspond to a Duffing oscillator having a linear resonant frequency of  $f_0=51\text{kHz}$  , a  $Q$ -factor of  $Q=1/(2\zeta_1)=1,515$  and a nondimensional cubic stiffness of  $\alpha=9,173$ .

Hence, for a given value of the forcing level,  $q$ , there exists a drop-down frequency, and as  $q$  increases, the drop-down frequency also increases. The drop-down frequency as a function of excitation force,  $q$ , is shown in Fig. b. Reconsidering now the case of base excitation, the forcing level is not fixed, but rather is proportional to the base excitation amplitude and the square of the drive frequency as seen in equation (1). Therefore, at a given base excitation amplitude, as the drive frequency is swept forward the corresponding forcing level also increases, yielding an increase of the drop-down frequency according to equation (6). The net effect is that, in the case of base excitation, as the drive frequency is swept forward, the drop-down frequency increases continuously, and for sufficiently large

base excitation amplitudes (i.e., above a critical threshold), the instantaneous drop-down frequency is always greater than the instantaneous drive frequency. The minimum base excitation amplitude required to achieve this effect is the critical excitation amplitude. A more detailed discussion of this phenomenon is presented in [16].

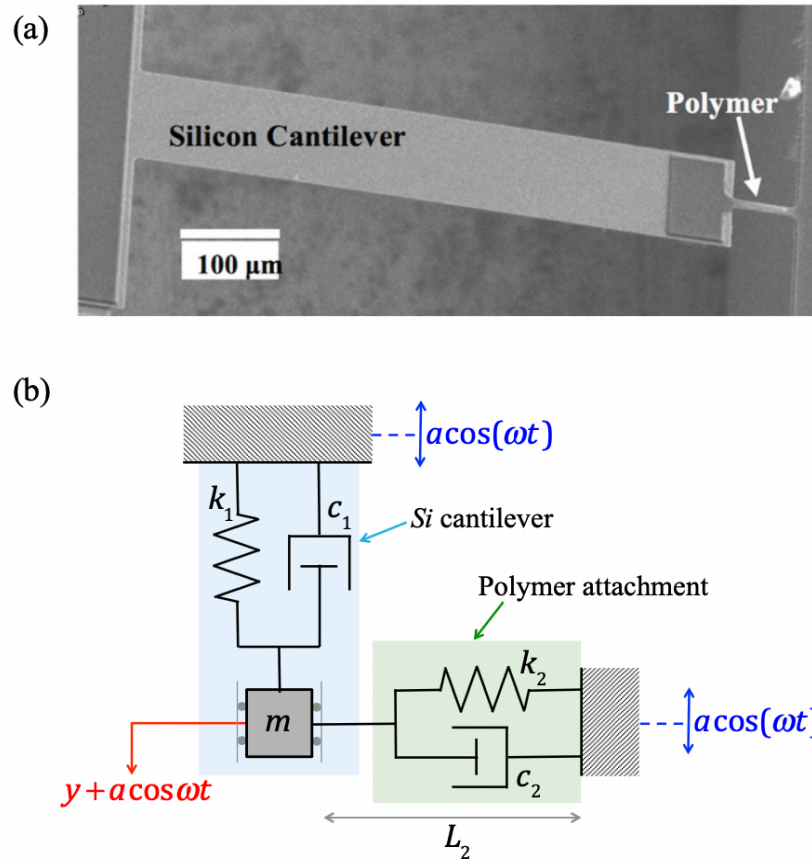


Figure 2: The experimental nonlinear microresonator: (a) An SEM image of the system [43] consisting of a Si micro cantilever grounded to the base via a polymer attachment; (b) The lumped parameter model of the system. The flexural motion of the Si cantilever is modeled by a linear damped harmonic oscillator with effective stiffness  $k_1$ , effective mass  $m$ , and effective damping coefficient  $c_1$ , where the displacement of the effective mass corresponds to the displacement of the tip of the cantilever. The effective mass is constrained by a horizontal viscoelastic element with stiffness  $k_2$  and damping coefficient  $c_2$ , which models the nonlinear effect of the polymer attachment. The large flexural displacement of the cantilever induces axial stretching in the polymer attachment resulting in geometric nonlinearity in the system's dynamics. The horizontal (nonlinear) damper does not play a significant role when  $y$  is relatively small and hence, the nonlinear damping is ignored in the theoretical reconstruction (see Fig. 3) within this dynamic regime. On the other hand, the vertical (linear) damper does not play a significant role when  $y$  is

*relatively large because the nonlinear damping effect is dominant and therefore, the linear damping is ignored within the large amplitude dynamic regime.*

### **III. EXPERIMENTAL RESULTS AND THEORETICAL RECONSTRUCTION**

To verify the theoretical predictions presented in Fig. 1, we experimentally investigate the dynamics of the device shown in Fig. 2 in a frequency range in the neighborhood of its fundamental bending mode. The system consists of a *Si* microcantilever that is connected by a polymer bridge to a fixed base. The nonlinear stretching of the polymer bridge resulting from the transverse motion of the tip of the microcantilever generates the desired nonlinear stiffness effects in this microresonator.

As discussed in a previous study in [43], by design the *Si* cantilever has a significantly lower bending stiffness than the polymer attachment and, as a result, transverse loading induces a relatively larger bending deflection of the *Si* cantilever as compared to the polymer attachment. Similarly, the axial stiffness of the polymer bridge is designed to be considerably smaller than that of the *Si* cantilever so that an axial force primarily stretches the polymer bridge and not the *Si* cantilever. As a result, harmonic excitation near the microcantilever's first bending mode induces large flexural motion of the *Si* cantilever and relatively large axial stretching of the polymer attachment. Accordingly, under harmonic excitation from the base, the *Si* cantilever behaves as a linear, damped SDOF harmonic oscillator, which is constrained in the transverse direction by a viscoelastic element (see Fig. 2b). Hence, in the frequency range considered in the experiment, the amplitudes of the higher cantilever modes are small and their effects on the measured dynamics negligible. Details regarding the fabrication of this device and experimental setup are presented in [43].

Moreover, it has been shown in [39, 43, 47] that the SDOF reduced-order model shown in Fig. 2b captures well the geometrically nonlinear effects due to the stretching of the polymer attachment. By applying either the Newtonian or Lagrangian method to the reduced order system depicted in Fig. 2b, and retaining only leading order nonlinear terms for small oscillations (i.e.,  $y/L \ll 1$ ), the following equation of motion is recovered,

$$m\ddot{y} + c_1\dot{y} + k_1y + k_3y^3 + c_3\dot{y}y^2 = ma\omega^2 \cos\omega t, \quad k_3 = \frac{k_2}{2L_2^2}, \quad c_3 = \frac{c_2}{L_2^2} \quad (5)$$

where the parameters used in equation (5) are defined in Fig. 2b. Specifically, as the effective mass  $m$  moves, the force imparted to the mass by the viscoelastic element representing the polymer attachment is an essentially nonlinear function (i.e. having no linear component) of the displacement  $y$ . To leading order, this force is of the form  $k_3y^3 + c_3\dot{y}y^2$ . On the other hand, the elastic and dissipative forces imparted on the mass by the lumped-parameter model representing the cantilever, are linear. As a result, when the microbeam system is harmonically driven from the base with an excitation amplitude of  $a$ , the equation of motion in (5) characterizes well the leading order dynamics of the microresonator in the neighborhood of the fundamental bending mode of the microcantilever. Finally, by introducing the following normalizations,

$$\hat{y} = \frac{y}{L_1}, \quad \tau = \omega_0 t, \quad ( )' = \frac{d}{d\tau}, \quad \omega_0 = \sqrt{\frac{k_1}{m}}, \quad \zeta_1 = \frac{c_1}{2m\omega_0} \quad (6)$$

$$\zeta_2 = \frac{c_3 L_1^2}{m\omega_0}, \quad \Omega = \frac{\omega}{\omega_0}, \quad \alpha = \frac{k_3 L_1^2}{m\omega_0^2}, \quad \hat{a} = \frac{a}{L_1}$$

equation (5) can be written in the following form,

$$\hat{y}'' + 2\zeta_1\hat{y}' + \hat{y} + \alpha\hat{y}^3 + \zeta_2\hat{y}'\hat{y}^2 = \hat{a}\Omega^2 \cos\Omega\tau \quad (7)$$

Note that equation (6) differs from equation (1) only in the presence of an additional nonlinear damping term proportional to the product of the velocity and the square of the displacement. The theoretical analysis showed that the combined effect of nonlinear hardening (i.e. forward bending of the resonance curve towards higher frequencies) and base excitation results in significant bandwidth expansion as the excitation amplitude approaches the critical level. Indeed, the microresonator of Fig. 2 has been shown to exhibit strong nonlinear hardening in the fundamental resonance [43]. Hence, it is

reasonable to expect the theoretically predicted ultra-broadband resonance of the microresonator (1) should also be exhibited by the experimental system of Fig. 2, under harmonic base excitation.

Aiming to experimentally verify the occurrence of the ultra-broadband resonance phenomenon due to geometric nonlinearities, we obtained experimental frequency response curves for this device at various constant excitation amplitudes. The specific device tested incorporates a  $500\ \mu\text{m} \times 100\ \mu\text{m} \times 20\ \mu\text{m}$  *Si* cantilever, and a  $40\ \mu\text{m} \times 20\ \mu\text{m} \times 3\ \mu\text{m}$  polymer attachment. A piezoelectric shaker attached to the base of the microbeam system was used to provide the required harmonic base excitation, and the shaker was carefully chosen so that the operational frequencies were well outside the resonance of the shaker. This allowed us to assume that the shaker responded linearly to the excitation. Concerning the prescribed base motion, the excitation of the shaker with a fixed voltage level corresponded to a fixed excitation amplitude of the resulting base oscillation, but not to a fixed forcing level. In fact, the resulting forcing level was proportional to the product of the drive frequency squared and the excitation amplitude (see the right-hand side of equation (5)). The shaker was excited with an AC voltage at peak-to-peak values ranging from 3V to 20V provided by a function generator. The dynamic response of the microbeam was measured by a laser Doppler vibrometer (LDV; Polytec OFV-534 sensor and OFV-5000 controller), with the laser pointed at the free end of the *Si* cantilever in order to measure its maximum transverse deflection. The measured signal was delivered to a computer via an oscilloscope (Tektronix DSOX4034A) where it was post-processed in LabView. The excitation frequency was incrementally swept forward, and for each value of the frequency, the numerical Fast Fourier Transform (FFT) of the steady-state motion of the cantilever tip was computed, and the measured amplitude at the fundamental harmonic digitally recorded.

(a)

(b)

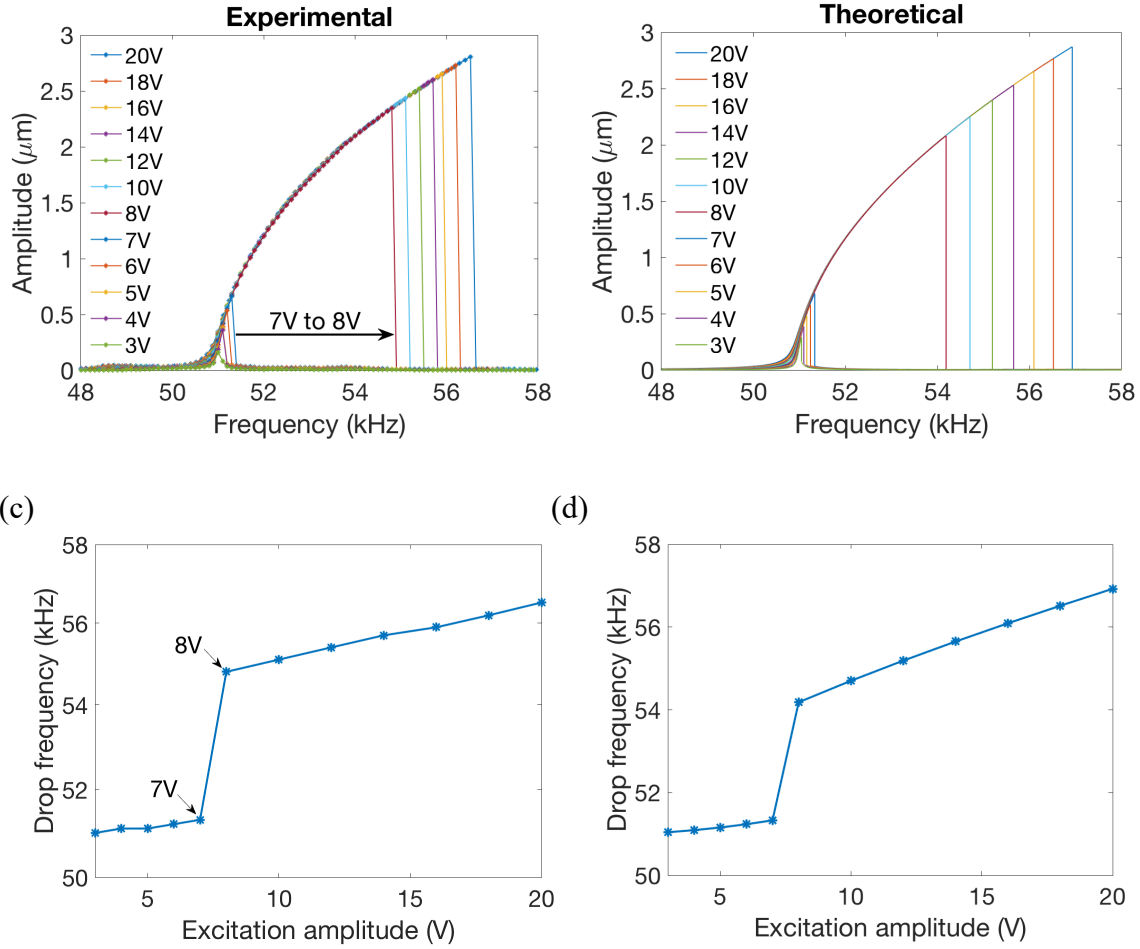


Figure 3: Experimental (a) and theoretically reconstructed (b) resonance curves (only forward sweeps) for varying excitation amplitudes in volts, and experimental (c) and theoretically reconstructed (d) drop-down frequencies as functions of excitation amplitude for the microresonator of Fig. 2. Note the ultra-broadband nonlinear resonance occurring at excitation voltages above 7V.

In Fig. 3a, the experimental resonance curves of the microresonator near its fundamental bending mode are shown and in Fig. 3c, the corresponding experimental drop-down frequency as a function of the excitation amplitude (in Volts) is shown. We start by performing a forward frequency sweeps at the fixed excitation voltage (amplitude) of 20V, which produces the experimental resonance curve at that excitation amplitude. Following that, we decrease the excitation voltage at the increments shown in the plot of Fig. 3a, performing similar forward sweeps at each (fixed) excitation amplitude. The smallest

voltage is 3V, at which point the microresonator behaves approximately linearly. We see that, as the excitation voltage increases from 3V to 7V, the drop-down frequency increases steadily, but from 7V to 8V, the drop-down frequency abruptly increases substantially; and from 8V to 20V, the drop-down frequency steadily increases but at a lower rate. The abrupt increase in the drop-down frequency between 7V and 8V caused by a small increase in the excitation voltage near 7V is evidence of the critical excitation amplitude that was theoretically predicted in Section II, denoting the initiation of ultra-broadband nonlinear resonance. Qualitatively similar results were observed for a different microresonator system having a  $500\ \mu\text{m} \times 100\ \mu\text{m} \times 20\ \mu\text{m}$  *Si* cantilever, and a  $40\ \mu\text{m} \times 20\ \mu\text{m} \times 3\ \mu\text{m}$  polymer attachment and are presented in the supporting information. It is important to note that no significant peak in the FFT of the steady-state motion was found other than the dominant peak at the drive frequency throughout all the experimental range. As such, internal resonance was not excited in any cases.

In a final step, we estimate the  $Q$ -factor, linear resonant frequency and nondimensional cubic stiffness in order to theoretically reconstruct the resonance curves. By theoretically fitting the experimental resonance curve at an excitation voltage of 0.1V (where the response is in the linear dynamics regime) the linear resonant frequency and  $Q$ -factor are simultaneously estimated to be  $f_0 = 51\text{kHz}$ , and  $Q = 1/(2\zeta_1) = 1,515$ , respectively. Further, by fitting the theoretical backbone to the experimental resonance curves below 8V, the nondimensional cubic stiffness is estimated to be  $\alpha = 9,173$ . Finally, by fitting the drop frequencies corresponding to excitation voltages between 3V and 7V using equation (4), the sensitivity of the piezo shaker was found to be 0.064nm/V. A detailed description of this fitting is presented in the supplementary material [48]. Note that because nonlinear damping does not play a role in the dynamics within the linear dynamic regime, the estimation of  $f_0$  and  $Q$  are independent of the nonlinear damping model. Additionally, since dissipative effects do not affect the backbone, the estimation of  $\alpha$  is independent of the damping model.

In order to reconstruct the forward frequency sweeps, we assume linear damping in the low-amplitude regime corresponding to excitation voltages of 3V to 7V, and assume a nonlinear damping model in the high-amplitude regime corresponding to excitation voltages of 8V-20V. Specifically, for excitation levels 8V to 20V, nonlinear damping of the form  $\zeta_2 \hat{y}' \hat{y}^2$  is imposed with  $\zeta_2 = 30$  (note this is the nonlinear damping model from (7)). In other words, a two-phase damping model is used to theoretically reconstruct the resonance curves in which linear damping is used when the oscillation amplitude is relatively small for excitation levels in the range 3V-7V while nonlinear damping of the form  $\zeta_2 \hat{y}' \hat{y}^2$  is used when the oscillation amplitude gets abruptly high in the range 8V-20V. The physical reason for this two-phase damping model is that the nonlinear damping does not play a significant role when  $y$  is small whereas the linear damping does not play a significant role when  $y$  is large (since the nonlinear damping effect is dominant). The theoretically reconstructed forward frequency sweeps and drop-down frequency as a function of excitation amplitude in volts, are shown in Figs. 3b and 3d. Here we see reasonable quantitative agreement with the corresponding experimental results shown in Figs. 3a and 3c.

#### IV. CONCLUSION

In a recent study [16] it was theoretically and computationally shown that a Duffing oscillator (i.e., an oscillator with cubic stiffness in addition to linear stiffness) subject to harmonic excitation applied to the base rather than as a body force can support ultra-broadband resonances owing to a newly reported nonlinear phenomenon termed the *no-drop phenomenon*. In contrast to direct force excitation, the forcing level is not fixed for base excitation, but rather is proportional to the product of the excitation amplitude and the drive frequency squared. It was shown by Potekin et al. (2018) that above a critical base excitation amplitude, there is no theoretically predicted drop-down bifurcation point in the resonance curve.

In this study, we experimentally investigated this phenomenon by considering the dynamics of a *Si* microcantilever restricted at its free end by a polymer bridge and subject to base harmonic excitation. It has previously been shown that in the frequency range close to the fundamental bending mode, strong hardening (i.e. forward bending) of the frequency response occurs due to geometric nonlinearity in the beam. Experimental resonance curves of this nonlinear microresonator at different excitation amplitudes were obtained. We observed an abrupt and significant increase in the resonant bandwidth above a certain critical excitation threshold. This signified the initiation of nonlinear ultra-broadband resonance in this device. Moreover, quantitative agreement was observed between the experimental resonance curves and the corresponding theoretically reconstructed curves.

Ultra-broadband resonances in micro-scale resonators are expected to be beneficial in many MEMS applications for signal processing, energy harvesting, sensing, RF electronics, and frequency control. There are several different ways one might go about increasing the bandwidth of a microresonator. For example, one can aim to reduce damping and/or increase the forcing level; however, these techniques have their limitations. The results shown in this paper along with the results presented in [16] illustrate an unconventional strategy for resonant bandwidth expansion in microresonators. Apart from enhanced MEMS applications, we anticipate that the nonlinear ultra-broadband phenomenon can be effective in diverse fields, e.g., in new types of nonlinear multi-frequency AFM measurement techniques, and nonlinear acoustic metamaterials with heretofore unattainable dynamical and acoustical properties.

## **ACKNOWLEDGEMENTS**

This work was financially supported in part by the National Science Foundation, Grant NSF CMMI 14-638558 at the University of Illinois at Urbana-Champaign, and Grant NSF CMMI-1619801 at The Ohio State University. This support is gratefully acknowledged. We also acknowledge Professor Junghoon Yeom, from the Department of Mechanical Engineering at Michigan State University, and his student Snehan Peshin for fabricating the microbeam resonator considered experimentally in this work.

## REFERENCES

- [1] O. Brand, I. Dufour, S. M. Heinrich, and F. Josse, *Resonant MEMS: Fundamentals, Implementation and Application* (Wiley-VCH Verlag GmbH & Co. KGaA, Weinheim, Germany, 2015).
- [2] K. L. Ekinici, Y. T. Yang, and M. L. Roukes, Ultimate limits to inertial mass sensing based upon nanoelectromechanical systems, *J. Appl. Phys.* **95**, 2682 (2004).
- [3] K. L. Ekinici and M. L. Roukes, Nanoelectromechanical systems, *Rev. Sci. Instrum.* **76**, 061101 (2005).
- [4] N. Kacem, J. Arcamone, F. Perez-Murano, and S. Hentz, Dynamic range enhancement of nonlinear nanomechanical resonant cantilevers for highly sensitive NEMS gas/mass sensor applications, *J. Micromechanics Microengineering* **20**, 45023 (2010).
- [5] K. Asadi, J. Yu, and H. Cho, Nonlinear couplings and energy transfers in micro- and nano-mechanical resonators: intermodal coupling, internal resonance and synchronization, *Phil. Trans. R. Soc. A* **376**, 0141 (2018).
- [6] R. Lifshitz and M. C. Cross, Nonlinear Dynamics of Nanomechanical and Micromechanical Resonators, In H. G. Schuster (Ed.), *Review of Nonlinear Dynamics and Complexity* (Wiley-VCH Verlag GmbH & Co. KGaA, Weinheim, Germany, 2008).
- [7] J. F. Rhoads, S. W. Shaw, and K. L. Turner, Nonlinear Dynamics and Its Applications in Micro- and Nanoresonators, *J. Dyn. Syst. Meas. Control* **132**, 34001 (2010).
- [8] M. I. Younis and F. Alsaleem, Exploration of New Concepts for Mass Detection in Electrostatically-Actuated Structures Based on Nonlinear Phenomena, *J. Comput. Nonlinear Dyn.* **4**, 21010 (2009).
- [9] A. H. Nayfeh and D. Mook, *Nonlinear Oscillations* (Wiley-VCH Verlag GmbH & Co. KGaA, Weinheim, Germany, 2004).
- [10] D. Antonio, D. H. Zanette, and D. López, Frequency stabilization in nonlinear micromechanical oscillators, *Nat. Commun.* **3**, 806 (2012).
- [11] N. Bajaj, A. B. Sabater, J. N. Hickey, G. T. C. Chiu, and J. F. J. Rhoads, Design and Implementation of a Tunable, Duffing-Like Electronic Resonator via Nonlinear Feedback, *J. Microelectromechanical Syst.* **25**, 2 (2016).
- [12] C. Chen, D. H. Zanette, J. R. Guest, D. A. Czapslewski, and D. López, Self-Sustained Micromechanical Oscillator with Linear Feedback, *Surface Science Letters* **117**, 017203 (2016).
- [13] P. Polunin, Y. Yang, J. Atalaya, E. Ng, S. Strachan, O. Shoshani, M. Dykman, S. Shaw and T. Kenny, Characterizing MEMS nonlinearities directly: The ring-down measurements, *Proc. Transducers 18th Int. Conf. Solid-State Sens. Actuators Microsyst. (TRANSDUCERS)*, 2176 (2015).
- [14] P. M. Polunin, Y. Yang, M. I. Dykman, T. W. Kenny, and S. W. Shaw, Characterization of MEMS Resonator Nonlinearities Using the Ringdown Response, *J. Microelectromech. Syst.* **25**, 297 (2016).
- [15] H. K. Lee, R. Melamud, S. Chandorkar, J. Salvia, S. Yoneoka, and T. W. Kenny, Stable Operation of MEMS Oscillators Far Above the Critical Vibration Amplitude in the Nonlinear Regime, *JMEMS* **20**, 1228 (2011).

- [16] R. Potekin, S. Kim, D. M. McFarland, L. A. Bergman, H. Cho, and A. F. Vakakis, A micromechanical mass sensing method based on amplitude tracking within an ultra-wide broadband resonance, *Nonlinear Dyn.* **92**, 287 (2018).
- [17] D. A. W. Barton, S. G. Burrow, and L. R. Clare, Energy Harvesting from Vibrations With a Nonlinear Oscillator, *J. Vib. Acoust.* **132**, 021009 (2019).
- [18] S. P. Beeby, Energy Harvesting Devices, In O. Brand, I. Dufour, S. M. Heinrich, and F. Josse (Eds.), *Resonant MEMS: Fundamentals, Implementation and Application* (Wiley-VCH Verlag GmbH & Co. KGaA, Weinheim, Germany, 2015).
- [19] M. Panyam and M. F. Daqaq, Characterizing the effective bandwidth of tri-stable energy harvesters, *J. Sound Vib.* **386**, 336 (2017).
- [20] D. Su, R. Zheng, K. Nakano, and M. P. Cartmell, Stabilisation of the high-energy orbit for a non-linear energy harvester with variable damping, *Proc. IMechE Part C: J. Mechanical Engineering Science* **230**, 2003 (2016).
- [21] A. Z. Hajjaj, A. Hafiz, and M. I. Younis, Mode Coupling and Nonlinear Resonances of MEMS Arch Resonators for Bandpass Filters, *Sci. Rep.* **7**, 41820 (2017).
- [22] S. Ilyas, K. N. Chappanda, and M. I. Younis, Exploiting nonlinearities of micro-machined resonators for filtering applications, *Appl. Phys. Lett.* **110**, 253508 (2017).
- [23] J. F. Rhoads, S. W. Shaw, K. L. Turner, and R. Baskaran, Tunable Microelectromechanical Filters that Exploit Parametric Resonance, *J. Vib. Acoust.* **127**, 423 (2005).
- [24] H. Askari, H. Jamshidifar, and B. Fidan, High resolution mass identification using nonlinear vibrations of nanoplates, *Measurement* **101**, 166 (2017).
- [25] A. Bouchaala, Jaber N., Shekhan O., Chernikova V., Eddaoudi M., and Younis M.I., Nonlinear-based MEMS sensors and active switches for gas detection, *Sensors* **16**, 758 (2016).
- [26] T. Hiller, L. L. Li, E. L. Holthoff, B. Bamieh, and K. L. Turner, System Identification, Design, and Implementation of Amplitude Feedback Control on a Nonlinear Parametric MEM Resonator for Trace Nerve Agent Sensing, *J. Microelectromechanical Syst.* **24**, 1275 (2015).
- [27] A. Jain, P. R. Nair, and M. A. Alam, Flexure-FET biosensor to break the fundamental sensitivity limits of nanobiosensors using nonlinear electromechanical coupling, *Proc. Natl. Acad. Sci.* **109**, 9304 (2012).
- [28] B. Jeong, C. Pettit, S. Dharmasena, H. Keum, J. Lee, J. Kim, S. Kim, D. M. McFarland, L. A. Bergman, A. F. Vakakis, Utilizing intentional internal resonance to achieve multi-harmonic atomic force microscopy., *Nanotechnology* **27**, 125501 (2016).
- [29] V. Kumar, J. W. Boley, Y. Yang, H. Ekowaluyo, J. K. Miller, T. -C Chiu., J. F. Rhoads, Bifurcation-based mass sensing using piezoelectrically-actuated microcantilevers, *Appl. Phys. Lett.*, **98**, 153510 (2011).
- [30] V. Kumar, Y. Yang, J. W. Boley, T. -C Chiu and J. F. Rhoads, Modeling, Analysis, and Experimental Validation of a Bifurcation-Based Microsensor, *J Microelectromech. Syst* **21**, 549 (2012).
- [31] L. L. Li, E. L. Holthoff, L. A. Shaw, C. B. Burgner and K. L. Noise squeezing controlled parametric bifurcation tracking of MIP-coated microbeam MEMS sensor for TNT explosive gas sensing, *J. Microelectromech. Syst.* **23**, 1228 (2014).
- [32] G. Prakash, A. Raman, J. Rhoads, and R. G. Reifenberger, Parametric noise

- squeezing and parametric resonance of microcantilevers in air and liquid environments, *Rev. Sci. Instrum.* **83**, 065109 (2012).
- [33] R. Potekin, S. Dharmasena, D. M. McFarland, L. A. Bergman, A. F. Vakakis, and H. Cho, Cantilever dynamics in higher-harmonic atomic force microscopy for enhanced material characterization, *Int. J. Solids Struct.*, **110**, 332 (2017).
- [34] R. Potekin, S. Dharmasena, H. Keum, X. Jiang, J. Lee, L. A. Bergman, A. F. Vakakis, and H. Cho., Multi-frequency Atomic Force Microscopy Based on Enhanced Internal Resonance of an Inner-Paddled Cantilever, *Sensors Actuators A Phys.* **273**, 206 (2018).
- [35] O. Shoshani, D. Heywood, Y. Yang, T. W. Kenny, and S. Shaw, Phase noise reduction in an MEMS oscillator using nonlinearly enhanced synchronization domain. *J Microelectromech. Syst.* **25**, 870 (2016).
- [36] L. G. Villanueva, R. B. Karabalin, M. H. Matheny, E. Kenig, M. C. Cross, and M. L. Roukes, A Nanoscale Parametric Feedback Oscillator, *Nano Lett.* **11**, 5054 (2011).
- [37] H. Cho, M. F. Yu, A. F. Vakakis, L. A. Bergman, and D. M. McFarland, Tunable, broadband nonlinear nanomechanical resonator, *Nano Lett.*, **10**, 1793 (2010).
- [38] H. Cho, M. F. Yu, A. F. Vakakis, L. A. Bergman, and D. M. McFarland, Dynamics of microcantilever integrated with geometric nonlinearity for stable and broadband nonlinear atomic force microscopy, *Surf. Sci. Lett.* **606**, L74 (2012).
- [39] H. Cho, B. Jeong, M. Yu, A. F. Vakakis, D. M. McFarland, and L. A. Bergman, International Journal of Solids and Structures Nonlinear hardening and softening resonances in micromechanical cantilever-nanotube systems originated from nanoscale geometric nonlinearities, *Int. J. Solids Struct.* **49**, 2059 (2012).
- [40] J. F. Rhoads, C. Guo, and G. K. Fedder, Parametrically Excited Micro- and Nanosystems, In O. Brand, I. Dufour, S. M. Heinrich, and F. Josse (Eds.), *Resonant MEMS: Fundamentals, Implementation and Application* (Wiley-VCH Verlag GmbH & Co. KGaA, Weinheim, Germany, 2015).
- [41] A. F. Vakakis, O. V. Gendelman, L. A. Bergman, D. M. McFarland, G. Kerschen, Y. S. Lee, *Nonlinear Targeted Energy Transfer in Mechanical and Structural Systems I* (Springer, 2008).
- [42] I. Kozinsky, H. W. C. Postma, O. Kogan, A. Husain, and M. L. Roukes, Basins of attraction of a nonlinear nanomechanical resonator, *Phys. Rev. Lett.* **99**, 8 (2007).
- [43] K. Asadi, J. Li, S. Peshin, J. Yeom, and H. Cho, Mechanism of geometric nonlinearity in a nonprismatic and heterogeneous microbeam resonator, *Phys. Rev. B* **96**, 20170141 (2017).
- [44] A. Eichler, J. Moser, J. Chaste, M. Zdrojek, and A. Bachtold, Nonlinear damping in mechanical resonators made from carbon nanotubes and graphene, *Nat. Nanotechnol.* **6**, 339 (2011).
- [45] B. Jeong, H. Cho, M. Yu, A. F. Vakakis, D. M. McFarland, and L. A. Bergman, Modeling and Measurement of Geometrically Nonlinear Damping in a Microcantilever Nanotube System, *ACS NANO*, **7**, 8547 (2013).
- [46] S. Zaitsev, O. Shtempluck, E. Buks, O. Gottlieb, Nonlinear damping in a micromechanical oscillator, *Nonlinear Dyn.* **67**, 859 (2012).
- [47] D. Andersen, Y. Starosvetsky, A. Vakakis, and L. Bergman, Dynamic instabilities in coupled oscillators induced by geometrically nonlinear damping, *Nonlinear Dyn.*

**67, 807 (2012).**

[48] See Supplemental Material at [URL will be inserted by publisher] for details regarding parameter estimation."

